Biochimica et Biophysica Acta 1827 (2013) 30–37

Contents lists available at SciVerse ScienceDirect

Biochimica et Biophysica Acta

journal homepage: www.elsevier.com/locate/bbabio

Molecular symmetry determines the mechanism of a very efficient ultrafast excitation-to-heat conversion in Ni-substituted chlorophylls

Mariusz Pilch [a], Alina Dudkowiak [b,*], Barbara Jurzyk [b], Jędrzej Łukasiewicz [b], Anna Susz [a,c], Grażyna Stochel [c], Leszek Fiedor [a,**]

[a] Faculty of Biochemistry, Biophysics and Biotechnology, Jagiellonian University, Gronostajowa 7, 30-387 Kraków, Poland
[b] Institute of Physics, Faculty of Technical Physics, Poznan University of Technology, Nieszawska 13a, 60-965 Poznań, Poland
[c] Faculty of Chemistry, Jagiellonian University, Ingardena 3, 30-060 Kraków, Poland

ARTICLE INFO

Article history:
Received 24 April 2012
Received in revised form 20 August 2012
Accepted 10 September 2012
Available online 17 September 2012

Keywords:
Metallochlorophyll
Ultrafast relaxation
Central metal ion bonding
Photoacoustics
Photocalorimetric reference

ABSTRACT

In the Ni-substituted chlorophylls, an ultrafast (<60 fs) deactivation channel is created, which is not present in Ni-porphyrins. This observation prompted us to investigate in detail the mechanism of excitation-to-heat conversion in Ni-substituted chlorophylls, experimentally, using time-resolved laser-induced optoacoustic spectroscopy, and theoretically, using group theory approach. The Ni-substituted chlorophylls show exceptional photostability and the optoacoustic measurements confirm the prompt and very efficient (100%) excitation-into-heat conversion in these complexes. Considering their excellent spectral properties and the loss-free excitation-into-heat conversion they are likely to become a new class of versatile photocalorimetric references. The curious features of the Ni-substituted chlorophylls originate from the symmetry of a ligand field created in the central cavity. The central $N-Ni^{2+}$ bonds, formed via the donation of two electrons from each of the sp^2 orbitals of two central nitrogens to an empty $s-d_{x^2-y^2}$ hybrid centered on Ni^{2+}, have a considerable covalent character. The extreme rate of excited state relaxation is then not due to a ladder of the metal centered *d*-states, often invoked in metalloporphyrins, but seems to result from a peculiar topology of the potential energy surface (a saddle-shaped crossing) due to the covalent character of the $N-Ni^{2+}$ bonds. This is confirmed by a strong $0\rightarrow0$ character of electronic transitions in these complexes indicating a similarity of their equilibrium geometries in the ground (S_0) and the excited states (both Q_X and Q_Y). The excitation energy is very efficiently converted into molecular vibrations and dissipated as heat, involving the central Ni^{2+}. These Ni-substituted pigments pose a fine exemplification of symmetry control over properties of excited states of transition metal complexes.

1. Introduction

Metal ions and their chelates play pivotal roles as active centers in many biological and man-made systems. Metalloporphyrins and chlorophylls (Chls) are prominent examples of such complexes in which the centrally chelated but coordinately unsaturated metal ions largely determine their functioning as well as their interactions. The catalytic activity of the former class of complexes is determined by the presence of the transition metal ions in the central cavity while in the photosynthetic pigments Chls, the central Mg^{2+} ion, a non-transition metal, serves mainly as a coordination center. The central Mg^{2+} only weakly perturbs the π-electron system and photophysical features of the chromophore, essential for photosynthesis [1–4]. The significance of the electronic inertness of Mg^{2+} becomes evident after its substitution with divalent transition metal ions, which give rise to entirely new photophysical characteristics of metallosubstituted Chls. Thus, due to the interactions between the delocalized π-electron system of the chelator (Chl macrocycle) and electrons on the unfilled *d* subshell, the redox activity as well as the coordination of axial ligands may be enhanced while the excited state lifetimes and photochemical activity are drastically reduced [3,5–10]. Yet, heavier metal ions may bring about the enhancement of intersystem crossing (ISC) in the complex due to an internal heavy atom effect [3,11–14]. Such new features, contributed e.g. by Pd^{2+} and Ni^{2+} as the central metal ions, can be exploited for practical applications of metallosubstituted pigments [15,16]. Thus, Pd-derivatives of bacteriochlorophyll a (BChla) show exceptional qualities as photosensitizers for photodynamic therapy and are currently undergoing clinical trials against prostate cancer [17,18]. In another derivative, the Ni-substituted BChla (Ni-BChla), an ultrafast relaxation of the excited state occurs within several tens of femtoseconds, being among the fastest processes of this type [6,8,19,20]. By analogy to Ni-substituted porphyrins, the ultrafast relaxation in Ni-BChla has been attributed to

* Corresponding author. Fax: +48 61 665 31 78.
** Corresponding author. Fax: +48 12 664 69 02.
E-mail addresses: alina.dudkowiak@put.poznan.pl (A. Dudkowiak), leszek.fiedor@uj.edu.pl (L. Fiedor).

0005-2728/$ – see front matter © 2012 Published by Elsevier B.V.
http://dx.doi.org/10.1016/j.bbabio.2012.09.007

the existence of a ladder of the π-electron and metal-centered excited states, lying below the lowest excited singlet state and creating an efficient path for the conversion of the excitation energy into heat [8]. Intriguingly, however, such an ultrafast (tens of femtosecond) deexcitation path has never been observed in extensively studied Ni-porphyrins [21–25]. We have applied this unique feature of Ni-BChla to the studies of intracomplex energy transfer in photosynthetic antenna. The introduction of the Ni-substituted pigment as the ultrafast excitation trap in the bacterial LH1 antenna served to estimate the physical size of the complex and revealed a large delocalization of excitons in this type of photosynthetic antennae [19,20].

The excited state dynamics in Ni-BChla have been thoroughly studied using time-resolved absorption and emission techniques [6,8,26]. None of these studies, however, explained the discrepancies between the ultrafast relaxation of excited states of Ni-substituted porphyrins and Ni-BChla. Given relatively minor structural differences between porphyrins and Chls, the absence of the femtosecond deactivation path in Ni-porphyrins is somewhat puzzling. Furthermore, it is not clear why, upon incorporation of Ni-BChla into the LH1 antenna, the femtosecond relaxation path becomes entirely dominating [19]. A similarly fast relaxation pathway has been previously found in Ni-BChla-substituted bacterial photosynthetic reaction centers [27]. These intriguing questions prompted us to combine theoretical and experimental approaches in the analysis of the electronic structure of Ni-substituted Chls and the physical mechanism of the extremely fast and efficient excitation-to-heat conversion in these complexes. We prepared a series of Ni-substituted Chls and their photophysical properties in various solvents were investigated using steady state absorption and emission spectroscopies. The solvent effects on the efficiency and kinetics of the excitation-into-heat conversion in Ni-substituted Chls were studied using time-resolved laser-induced optoacoustic spectroscopy (LIOAS). In parallel, in order to gain deeper insights into the mechanism of these processes we have applied the group theory approach in the analysis of the symmetry properties of Ni-substituted Chls and their consequences for the peculiar behavior of these complexes.

2. Materials and methods

2.1. Pigment preparation

Chlorophylls a and b were extracted from frozen spinach leaves using methanol following a method described by Iriyama [28]. The pigments were purified first by column chromatography on Sepharose CL-6B (Sigma, Germany) using 1.5% (Chla) and 10% (Chlb) of 2-propanol in n-hexane as the eluent [29] and finally by isocratic HPLC in methanol on a Varian Microsorb 100-5 C-18 column (250×10.0 mm). BChla was isolated from the wet cells of *Rhodobacter sphaeroides* and purified on diethylaminoethyl (DEAE) Sepharose CL-6B (Sigma, Germany) as previously described [29] and then by HPLC on a Varian Microsorb 100-5 Si column (250×10.0 mm) using a 97:3 (v/v) mixture of hexane and 2-propanol as the eluent [30].

The metal free derivatives, pheophytin a (Phea), pheophytin b (Pheb) and bacteriopheophytin a (BPhea) were prepared from the respective pure Mg complexes by demetalation in doubly distilled glacial acetic acid [30]. The acid was removed in a stream of nitrogen and the solid residue was dried under vacuum and quickly purified by column chromatography either on DEAE-Sepharose CL-6B (BPhea) or on CM-Sepharose (Pharmacia, Uppsala, Sweden) (Phea and Pheb) in acetone. The purified pigments were thoroughly dried under vacuum and stored under Ar at −30 °C.

2.2. Metalation

The synthesis of Ni-Chla and Ni-Chlb were done via direct metalation of the respective pheophytins with a 10-fold excess of $Ni(OAc)_2$ (Alfa-Ventron, Danvers, MA) in doubly distilled glacial acetic acid for 40 min (Ni-Chla) or 240 min (Ni-Chlb) at 80 °C. Reaction progress was monitored by collecting small aliquots of the reaction mixtures, dissolving them in methanol and measuring their absorption spectra, and by TLC on cellulose (Whatman, UK). After removing the solvent in a stream of nitrogen, the product was isolated by column chromatography on CM-Sepharose CL-6B, using 10% MeOH in acetone (v/v) as the eluent. The final purification was done by isocratic HPLC on a reversed-phase silica gel (Varian Microsorb 100-5 C-18, 250×10.0 mm) using methanol as the eluent. The purified pigments were thoroughly dried under vacuum and stored under Ar at −30 °C.

Ni-BChla was prepared by the transmetalation method as described previously [7]. First, the precursor Cd-BChla complex was prepared by refluxing BPhea in dimethylformamide with anhydrous $Cd(OAc)_2$ and subsequent purification on silica gel. The addition of $NiCl_2$ to a solution of Cd-BChla in acetone yielded Ni-BChla. The product was initially isolated on Silica gel 60 (Merck) and finally by isocratic HPLC on a reversed-phase silica gel (Varian Microsorb 100-5 C-18, 250×10.0 mm) using methanol as the eluent.

2.3. Photostability study

The pigments were dissolved in 2 ml of absolute ethanol (Merck) to obtain solutions with absorbance equal to 0.5 at the Q_Y maximum. The solutions in equilibrium with air were stirred using a magnetic stirrer and irradiated with red light from a halogen light source (Schott LCD KL 1500) equipped with fiber optics, a water heat filter and a cut off filter RG 630 (Schott, $\lambda \geq 630$ nm). The light intensity used in the experiment was 31.2 mW cm^{-2}, as measured with a Field MaxII-TO light power meter (Coherent, USA). In all cases, the irradiation time was 120 min and the temperature of solutions was stabilized at 293 K, using a thermostated cuvette holder (MTC-R1, MedSon, Poland) placed inside the sample compartment of a Cary 50 spectrophotometer. The progress of pigment photodegradation was monitored by recording the absorption spectra of the samples during irradiation.

2.4. Spectroscopic measurements

The electronic absorption spectra were recorded using Cary 50 and 5000 spectrophotometers (Varian, USA). The emission spectra were measured on a Hitachi F-4500 fluorometer. The laser-induced laser-induced optoacoustic spectroscopy (LIOAS) method has been described in detail elsewhere [31,32]. To measure the heat generated as a result of light energy absorption, a nitrogen-dye laser (Photon Technology Int'l, GL-3300/GL-301) as the excitation source and a piezoelectric transducer (1 MHz, V103, Panametric, Inc., USA) as the detection system was applied. The laser pulse energy was monitored by splitting part of the beam to a pyroelectric energy probe (RjP-735) connected to an energy meter (Rj-7620). The signal was recorded on an oscilloscope (GoldStar OS-3060) for a 0–32 μJ energy range obtained by introducing optical gray filters in the laser beam path. The absorbances of samples were kept between 0.05 and 0.65. The measurements were carried out in air or argon atmosphere at room temperature with the samples placed in a thermostatic compartment (Flash 100). For each measurement 64 signals were averaged to increase the signal-to-noise ratio. To analyze the LIOAS signals home-made acquisition and Sound Analysis (1.50D) programs were used.

The parameter α is the fraction of absorbed energy released promptly as heat and it is related to an effective acoustic transit time defined as $\tau_a' = 2R/v_a$ (where $2R$ is the beam diameter (controlled by 1 mm pin hole) and v_a is the sound velocity in the solvent used) [33]. The value of α can be obtained by systematic measurements of H_{max} as a function of E_{las} and A for both the sample and the reference. In our experiments, depending on the solvent used,

the sound velocity (Table 1) changes from 1.00×10^3 m/s (in methanol) to 1.30×10^3 m/s (in acetonitrile), so τ_a' varies from 0.8 μs to 1.0 μs. As shown previously, [33,34] the transducer integrates the heat released in processes faster than roughly $\tau_a'/5$ (150–200 ns) and ignores all processes slower than $5\tau_a'$. Below $\tau_a'/5$ the amplitude wave is proportional to the heat released but if the photoproducts with a long lifetime are formed they can be detected in the intermediate $\tau_a'/5 \le \tau \le 5\tau_a'$ region.

For the measurements, the pigments were dissolved in different organic solvents such as acetone, acetonitrile, ethanol, methanol, pyridine and toluene (from POCH, Lublin, Poland or Sigma-Aldrich). The relevant physical properties of the solvents are listed in Table 1. Ferrocene (Sigma-Aldrich) was used as the photocalorimetric reference (PCR).

3. Results and discussion

3.1. Electronic absorption and emission

The electronic absorption spectra of Chla, Chlb and BChla, of their Ni-substituted analogs, and solvent effects on the spectra are shown in Fig. 1. In the spectra of both Ni-substituted Chla and Chlb, when compared to the parental pigments, the Soret and Q_Y bands become broader and undergo a blue shift of about 20 nm. In the case of BChla, the B component of the Soret band is shifted to the blue while the Q_Y band becomes broader and slightly red shifted, as seen previously [7]. The energies and intensities of major transitions in the absorption spectra of the Ni-substituted pigments show a weak solvent dependence; only in pyridine are larger shifts observed accompanied by changes of band intensities (Fig. 1). The intensity of the vibrational side bands, which usually accompany on the high energy sides the Q_Y transitions of Chls and also the Q_X band in BChla [35,36], seem to be reduced as indicated by the deconvolution analysis (not shown). Again, in pyridine the spectra do not follow this common pattern and the Soret and Q_Y bands experience larger shifts, whereas the vibrational side bands regain their intensity. The shifts of the Soret and Q_Y bands in pyridine are apparently related to the change in the axial ligation state of the central Ni^{2+} rather than to solvation effects; the same changes are observed also in weakly coordinating solvents containing pyridine (or imidazole) at very low concentrations, in the range of tens of μM (not shown). The central Ni^{2+} ion readily accepts two pyridines as axial ligands, as indicated by a characteristic shift of the Q_X energy in Ni-BChla (~600 nm, Fig. 1C) and the strong ligation by pyridine causes the complex to become paramagnetic [7,37].

The results of the emission measurements are summarized in Table 1. Similarly to Ni-BChla [6], the Ni-substituted Chla and Chlb show practically no emission of fluorescence. The lack of fluorescence emission indicates a strong competition between the radiative and fast nonradiative channels of excited state relaxation [6,19,27,37].

Table 1
Photophysical parameters of Ni-Chla in a series of organic solvents and the relevant properties of the solvents (where: η—solvent viscosity; $[O_2]$—oxygen concentration in air-saturated solvent; v_a—sound velocity in solvent; Φ_F—fluorescence quantum yield determined using Chla as a reference in methanol ($\Phi_F=0.32$); α_S—defined in Eq. (2)).

Solvent	η [42] 10^{-3} (Pa·s)	$[O_2]$ [43] 10^{-3} M	v_a [33] 10^3 m/s	Φ_F (±0.005)	α_S (±0.05)
Acetonitrile	0.345	1.68	1.30	0.00	1.07
Methanol	0.551	2.12	1.00	0.00	1.06
Ethanol	1.078	2.07	1.01	0.00	1.08
Acetone	0.304	2.40	1.05	0.00	1.05
Pyridine	0.883	–	–	0.00	0.98
Toluene	0.590	1.81	1.17	0.00	1.06

3.2. Optoacoustic measurements (LIOAS)

Time-resolved laser-induced optoacoustic spectroscopy was applied in order to estimate the efficiency of excitation-to-heat conversion in the Ni-substituted Chls, the kind of information not available from other techniques. The first maximum in the LIOAS signal, H_{max}, is proportional to the heat released to the environment from the excited sample on a short time scale [33,38]. The amplitude of H_{max} depends on the energy of the laser pulse (E_{las}) and the absorbance (A) of the sample in the following way:

$$H_{max} = K\alpha E_{las}\left(1-10^{-A}\right) \quad (1)$$

where K is a constant related to the geometry of the experimental setup and the thermoelastic properties of the medium, and α is the fraction of the absorbed energy released as prompt heat. The latter coefficient reflects the efficiency of the conversion of excitation energy into heat while the $1–10^{-A}$ factor describes the fraction of the incident light absorbed by the sample. To eliminate the unknown K, a photocalorimetric reference is usually applied, which with a 100% efficiency ($\alpha_R=1$) converts the absorbed energy into heat within a time much shorter than the time resolution of the experimental setup. K can be eliminated when the sample and the PCR are measured under identical conditions and the plot of H_{max} versus the incident laser energy multiplied by the fraction of energy absorbed yields a straight line. Since α_R and the absorbances of the sample (A_S) and the reference solution (A_R) are known, the fraction of the absorbed energy released by the sample as prompt heat (α_S) can be expressed as:

$$\alpha_S = \alpha_R \frac{H^S_{max}E^R_{las}\left(1-10^{-A_R}\right)}{H^R_{max}E^S_{las}\left(1-10^{-A_S}\right)} \quad (2)$$

A series of ferrocene (FC), a widely accepted PCR [39], and Ni-Chla solutions of the same absorbances at the excitation wavelength were measured under identical conditions. The measurements were conducted in a set of solvents in which the solubility of both pigments is relatively high and they remain in a monomeric state. Thus, in the entire range of Ni-Chl concentrations, the ratios of the intensities of the Soret and Q_Y bands did not change and the solutions obeyed the Beer–Lambert law (not shown).

The functional dependence of H_{max} on E_{las} and $(1–10^{-A})$ was verified in two ways, by varying the laser energy and the pigment concentration. The highest energy used in this work (about 32 μJ/pulse) was in the range commonly used in time-resolved pulsed photoacoustic experiments. The plots of the H_{max} amplitude of Ni-Chla in acetone as a function of E_{las} are shown in Fig. 2. The linearity of the signal was well reproduced at several excitation wavelengths (370, 406 and 640 nm) across the absorption spectrum of the pigment over the entire range of incident pulse energies. Practically the same results were obtained in other solvents (not shown), indicating that the H_{max} is solvent independent and that there is no interference between solvent–solute interactions and the relaxation processes in Ni-Chla.

The values of the α_S parameter were determined for the Ni-derivative in all solvents in the linear response region (Fig. 3), using the same PCR. In all cases, the value of α_S equals 1 within experimental error (Table 1). The constancy of α_S indicates that the thermal properties of Ni-Chl are independent of the physical properties of the medium. Some slightly overestimated α_S values may be related to the presence of PCR at high concentration (see below).

The values of α_S for Ni-Chla determined in Ar-saturated acetone (not shown) were similar to those obtained in the air-equilibrated solution (Table 1). No phase shift between the optoacoustic waveforms from Ni-Chla and FC was observed (not shown) with respect to the signals recorded in air-saturated solutions. This indicates that neither

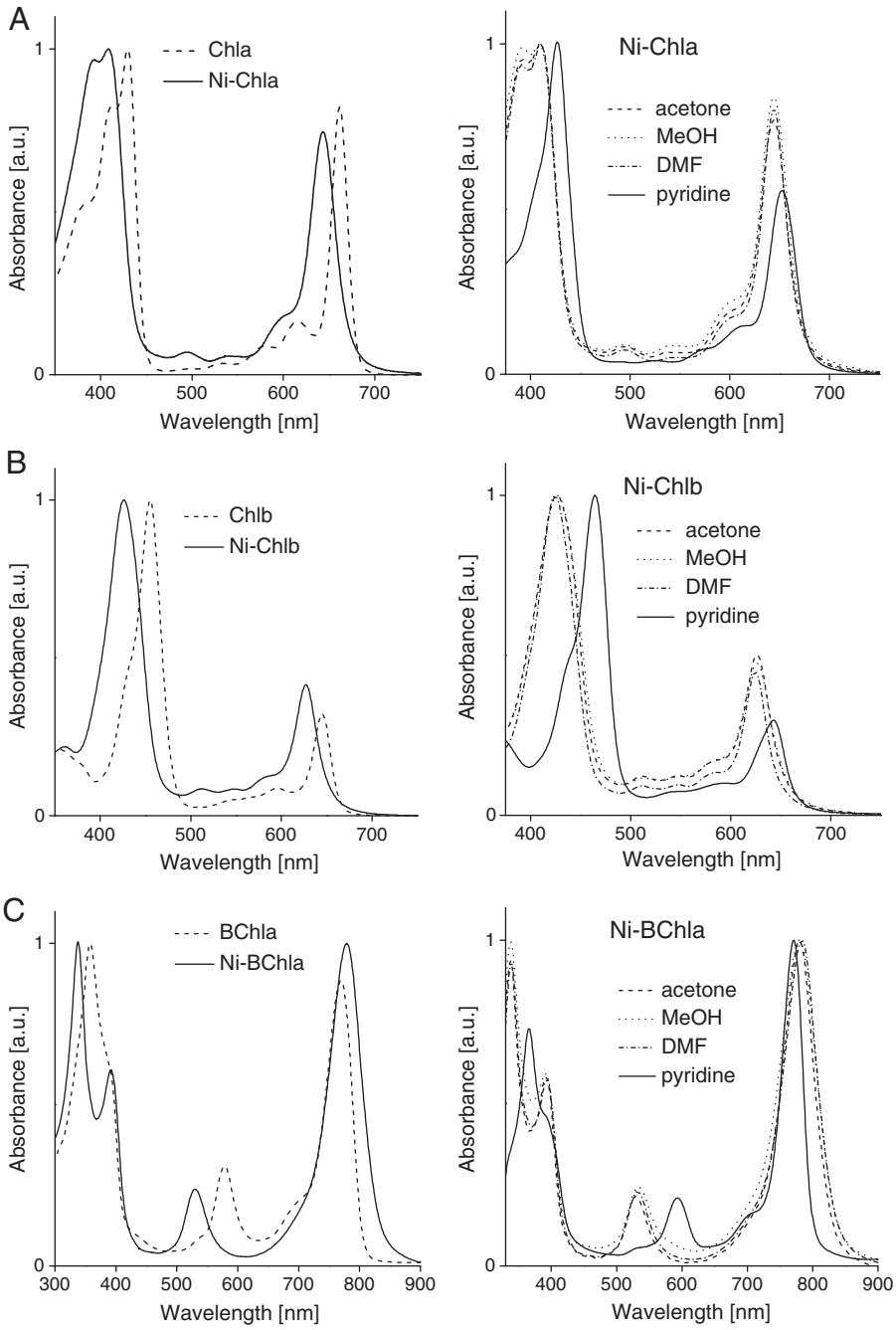

Fig 1. Electronic absorption spectra of chlorophyll a, chlorophyll b and bacteriochlorophyll a and their Ni-substituted derivatives recorded in acetonitrile (panels on the left). In the right panels, the spectra of the Ni-substituted derivatives recorded in acetone, methanol, dimethylformamide (DMF) and pyridine are shown. All spectra were taken at room temperature and were normalized to the most intensive bands.

transients, e.g. excited triplet states, with lifetimes longer than the ones observed in air-saturated solution are formed, nor does triplet–triplet energy transfer from the excited pigment to molecular oxygen occur.

From the analysis of the LIOAS profiles it follows that the efficiency of the excited state depopulation is constant in Ni-Chla, irrespective of oxygen content in the medium. Chls in a monomeric state are good photosensitizers due to an efficient intersystem crossing [40,41], even in the absence of heavy atoms, and such moderately heavy central atoms as Ni and Zn do not significantly enhance intersystem crossing [3,9]. This suggests that in the Ni-substituted complexes a loss-free conversion of excitation energy into heat is an entirely dominating process, which reduces the competitiveness of intersystem crossing.

3.3. Ni-substituted chlorophylls as a novel photocalorimetric reference

As mentioned, the reliability of the LIOAS technique rests on the availability of an appropriate PCR, a photochemically stable substance which upon excitation releases heat within a time shorter than the time resolution of the experimental set-up. Also, a calibration of the setup is required to determine the quantitative relationships between its response and the heat released [33,38]. A good PCR is expected to

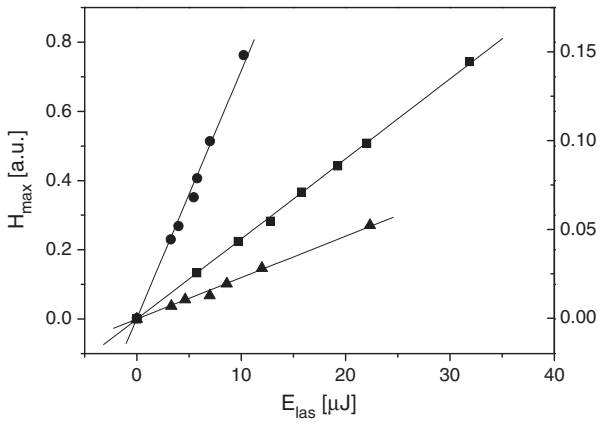

Fig. 2. Dependence of the LIOAS signal (H_{max}) from Ni-Chla in acetone on incident laser energy E_{las}, recorded at three excitation wavelengths: 370 (▲), 406 (■) (scale on the left) and 640 (●) nm (scale on the right). The absorbance of the sample was set to 0.1 at 406 nm.

have an absorption spectrum well overlapping that of the pigment being examined, and it cannot show any radiative relaxation of the excited state, thereby delivering all absorbed energy to the environment promptly as heat. The PCR and the sample should be measured under identical conditions, including the geometrical parameters of the experimental setup, the absorbance at the excitation wavelengths, etc. And, in particular, they have to be measured in the same medium because the signal is related to the time evolution of the pressure changes (wave) in a liquid sample, whose intensity depends on the solvent thermoelastic properties. Hence, there is a need for more versatile and solvent-insensitive PCRs. However, most of the references currently in use are inorganic salts or metalloorganics of low molar absorption coefficients and limited solubility, often being toxic and usable only over a narrow spectral range [33]. For instance, FC is widely accepted as a PCR for measurements in organic solvents [39] but its use is limited to the spectral regions covered by its absorption bands. Moreover, its molar absorption coefficient is fairly low (3.1×10^{1} M^{-1} cm^{-1} at 355 nm in acetonitrile [39]) and in order to obtain solutions with an absorbance near 0.1, it has to be used at considerably high concentrations, in the range of 10^{-3} M. Solutes at such concentrations can significantly affect the thermoelastic parameters of the solutions. In this respect, Ni-substituted Chls seem to be a much better choice. Thanks to their very high extinction coefficients, in the range of 7×10^{4} M^{-1} cm^{-1}, they can be applied at very low concentrations (~10^{-6} M), far below the threshold which would affect the thermoelastic properties of the medium or where pigment–pigment interactions would be induced that would influence thermal deactivation processes. The limits of the use of Ni-Chla as a PCR are indicated as non-linearities in the plots in Fig. 3, which only appear for the E_{las} and $(1–10^{-A})$ product as high as 15.0.

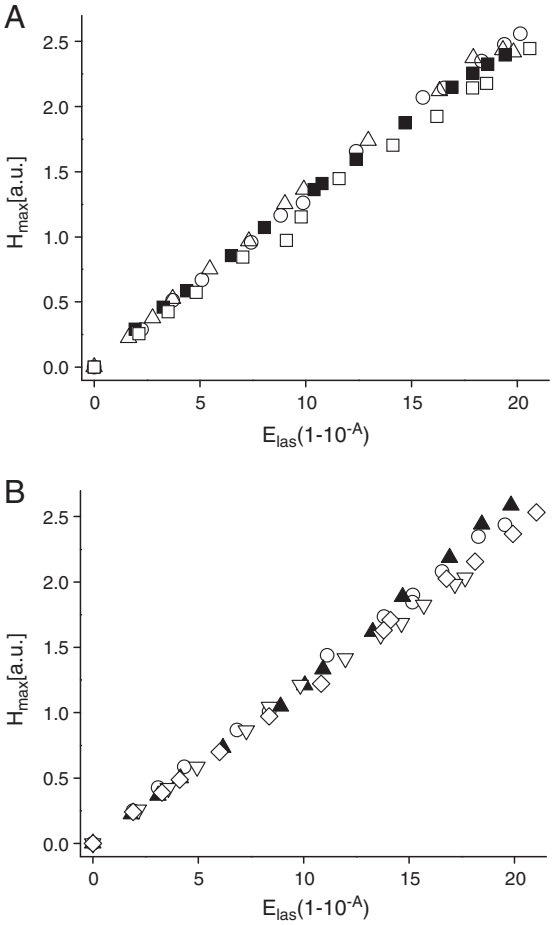

Fig. 3. Comparison of the amplitudes of the LIOAS signals (H_{max}) from ferrocene (solid symbols) and Ni-Chla (empty symbols) as a function of incident laser energy (at λ_{exc} = 406 nm) multiplied by the fraction of absorbed energy, estimated according to Eq. (1), in a series of solvents: (A) acetonitrile (○), ethanol (Δ) and methanol (□), and (B) acetone (○), toluene (Δ) and pyridine (□).

In terms of chemical and photochemical stability Ni-substituted Chls are also advantageous. The absorption spectrum (and absorbance) of an acetone solution of Ni-Chla changed by 7% over three months storage at 4 °C in the dark in the presence of oxygen. The effect of the central Ni^{2+} on the photostability was assessed in a comparative study on Chla, Chlb and BChla, and their Ni-substituted analogs. Pigments in ethanol were irradiated with red light ($\lambda \geq 630$ nm) for several hours at room temperature, in equilibrium with air, and their decay was monitored by recording the absorption spectra. Irradiation causes a quick bleaching of the Mg complexes while the Ni complexes show almost no photodegradation (Fig. 4). This confirms the excellent photostability of these complexes.

In conclusion, Ni-substituted Chls can be used as a very photostable and reliable PCR in a range of organic solvents, applicable at very low concentrations. Furthermore, since the major absorption transitions in Ni-Chls cover the range from 300 to 470 nm (Soret) and 620 to 790 nm (Q_Y), in terms of the excitation wavelength their applicability to the photoacoustic methodology extends far beyond any other PCRs. These features render Ni-substituted Chls superior to most PCRs currently in use.

3.4. Mechanism of excited state relaxation in Ni-BChla

There are several mechanisms which cause a shortening of excited state lifetimes of porphyrins. For instance, the distortions reduce the $^1(\pi,\pi^*)$ state lifetime from several tens of nanoseconds to around 1 ns, accompanied by an increase in the efficiency of the non-radiative relaxation [44]. Also, the conformational/vibrational relaxation in dodecaphenylporphyrin was shown to occur in ~10 ps time scale [45] and in free base porphycenes and substituted porphyrins [46] while an even shorter lifetime of the $^1(\pi,\pi^*)$ state, ~1 ps, was observed in distorted Ni-dodecaphenylporphyrin, followed by a slower relaxation of the (d,d^*) state [21]. Yet, the dynamics of the excited state relaxation in Ni-BChla, reaching 100–150 fs in solution [8] and even below 60 fs in LH1 antenna [19], is one order of magnitude faster, in the range of tens of femtoseconds, which is as fast as the intra-state vibrational redistribution in porphyrins [46]. Such an extreme rate of ground state recovery implies that another, exceptionally efficient, mechanism of excitation-to-heat conversion is active in Ni-(B)Chls, dominating all other possible routes of excited state relaxation. Its time scale excludes any significant contribution of ISC to this

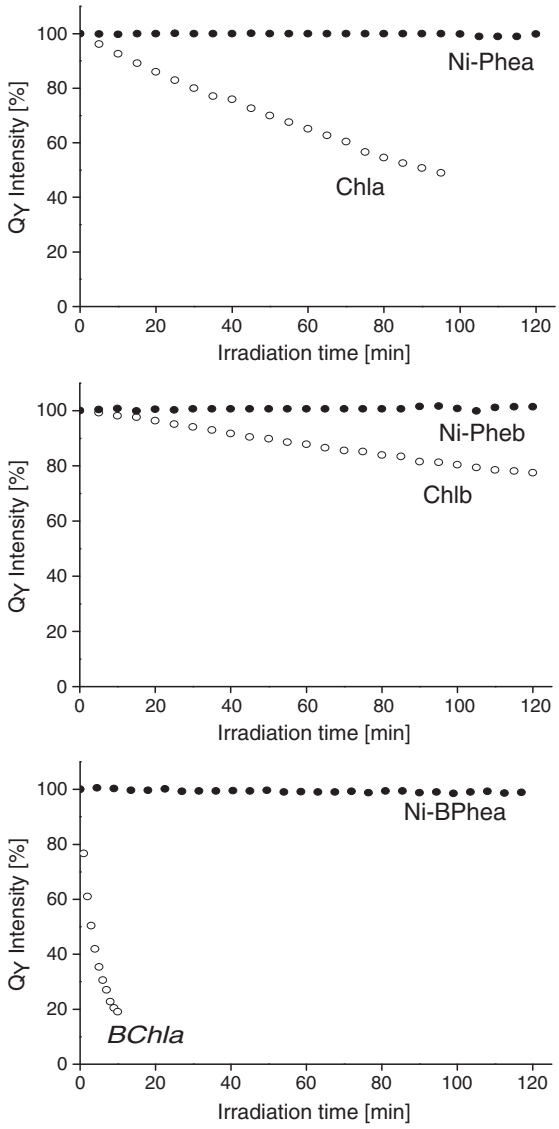

Fig. 4. Photostability of chlorophyll a, chlorophyll b and bacteriochlorophyll a and their Ni-substituted analogs in ethanol, shown as the decay of their Q_Y bands upon irradiation with red light (see the text for details).

process [3], as confirmed by the LIOAS measurements. Any plausible mechanism for excited state deactivation in Ni-substituted (B)Chls has to consider the interactions between the central Ni^{2+} ion and the chelating macrocycle. In contrast to simple porphyrins (D_{4h} symmetry), the ligand field in the central pocket of (B)Chls (effective C_{2h} symmetry, Fig. 5) is created by nonequivalent nitrogen atoms [47]. In the C_{2h} point group, the σ-bonds can be formed only by orbitals of b_u and a_g symmetry whereas the π-bonds only by orbitals of a_u symmetry [48]. The valence orbitals of the central nitrogens belong to both subsystems; p_z belongs to the π-system while the hybrid orbitals sp^2 belong to the σ-system. Two of these hybrids are involved in σ-bonding to carbon atoms and one hybrid protrudes into the metal binding pocket. In the same point group, the valence orbitals of the Ni^{2+} ion belong to the following irreducible representations, a_g ($s, d_{x^2-y^2}, d_{z^2} d_{xy}$), b_g (d_{xz}, d_{yz}), a_u (p_z) and b_u (p_x, p_y). The s, d_{z^2}, d_{xy}, and $d_{x^2-y^2}$ orbitals comprise the basis for four effective linear combinations:

$$\chi_i = c_{1i}(4s) + c_{2i}\left(3d_{xy}\right) + c_{3i}(3d_{z^2}) + c_{4i}\left(3d_{x^2-y^2}\right) \quad (3)$$

where $i = 1, 2, 3$ and 4.

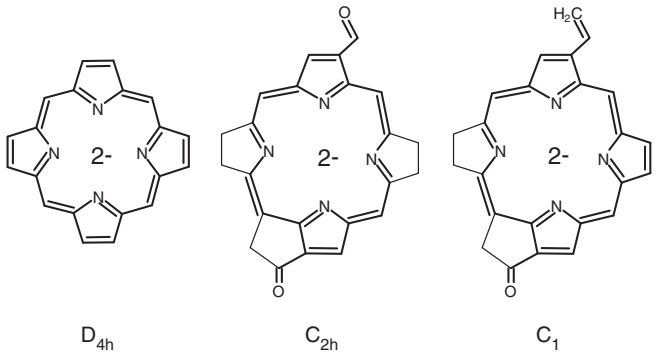

Fig. 5. Assignment of symmetry point groups to anionic forms of porphyrin and its two reduced derivatives comprising the skeleton of bacteriochlorophyll a and chlorophyll a, respectively. The conjugated p-electron system is indicated in bold.

Similarly to Ni-porphyrins [49], the 4*s* and one of the 3*d* orbitals of the Ni^{2+} ion form two $\chi_\pm = \frac{1}{\sqrt{2}}(3d_{x^2-y^2} \pm 4s)$ hybrids which accommodate four electrons from the central nitrogens (see Fig. 6).

The central metal–N bonds can then be described as $\phi_\pm = sp^2(N) + \chi_\pm$, with higher electron density on the χ_+ hybrid. The system of these two (oscillating) bonds may be viewed as a three-center-bond N_{21}-Ni^{2+}-N_{23} (the IUPAC numbering system) of a considerably covalent character. At the same time, as in Ni-porphyrins [48,49], one would expect an unfavorable interaction (repelling) to occur between the lone pair electrons (sp^2) on the N_{22} and N_{24} atoms and electrons localized on the d_{xy} orbital, in line with the fact that often in Ni-porphyrins the central ion is slightly shifted above the complex plane [21,23]. In the C_2 group (Ni-BChla), also the p_z(Ni) orbital may contribute to the linear combination χ_i. The resultant exceptionally strong chelation of Ni^{2+} in the central pocket of (B)Chls is in line with a very high, as compared to the Mg complexes, chemical stability of the Ni-substituted tetrapyrroles [7,10,48,49].

The changes in the absorption spectra of the Ni-substituted pigments indicate changes in the molecular vibrations due to the enhanced covalent character of the metal ion–N bonding. As shown in Fig. 1, the vibrational sidebands of both the Q_X and Q_Y transitions, characteristic of Mg complexes [2,36,50], in particular in Ni-BChla, lose their intensity and both transitions seem to have a strong $0 \rightarrow 0$ character. Intriguingly, the sidebands reappear in the spectrum of Ni-BChla in pyridine (Fig. 1C), in line with the notion that the N – Ni

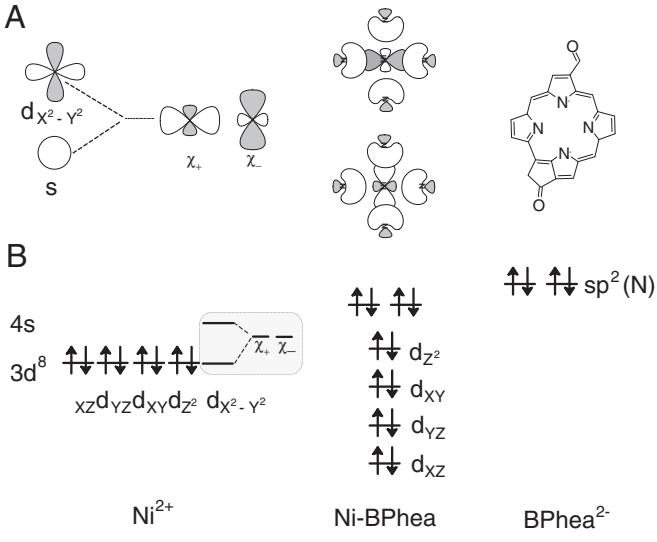

Fig. 6. Schematic presentation of (A) interacting orbitals of Ni^{2+} ion and bacteriopheophytin (BPhe) macrocycle in the complex (no axial ligands present), and (B) the electron occupancy of the orbitals involved, assuming the ligand field of C_{2h}/C_1 symmetry.

bonding to the in-plane located hexacoordinated central Ni^{2+} ion must be weakened due to an unfavorable orbital overlap, as discussed above.

In Ni-porphyrins, the rapid excited state relaxation is known to occur via internal conversion (IC) followed by vibrational relaxation of the metal centered excited *d*-states [22–25,51,52]. However, the ladder of *d* substates in Ni-(B)Chls is not really feasible because formally there are no vacant *d* levels (see Fig. 6). Furthermore, a strong $0 \rightarrow 0$ character of electronic transitions in these complexes (Fig. 1) implies that their equilibrium geometries in the ground (S_0) and the excited states (both Q_X and Q_Y) are similar and that transitions to other oscillating states ($0 \rightarrow 1$, $0 \rightarrow 2$, etc.) have lower probability.

In light of the above, we propose that the oscillation of the central Ni^{2+} facilitate the prompt conversion of excitation energy into the kinetic/potential energy of the central Ni, creating a very rapid route for the relaxation. In the excited states electron density grows on the pairs of diagonally located N atoms [53] and thus the central ion is pulled down into the macrocycle plane (change of symmetry $C_2 \rightarrow C_{2h}$). This, in turn, destabilizes the $Ni^{2+}-N$ bonds (see above) and the excitation energy is converted to the potential energy of a dumped-oscillating ion. The proposed relaxation pathway would involve the transmission of vibrations to the strongly chelating central nitrogens as well. In the presence of axial ligand(s), such a pathway may become even more efficient, as the excess energy can be dissipated to the surrounding via vibrations of the ligand(s) [8,22,54]. Seemingly, the mass of the central ion is the major factor which determines the rate of energy dissipation because a similarly fast and efficient conversion of excitation energy into heat has been observed in the complexes of Co and Fe [55–57]. Apparently, if the central ion were heavier (e.g. Pd, Pt) it would be more difficult to tilt it from equilibrium position and the excitation energy could not be dissipated as quickly. This is in line with indeed longer excited state lifetimes in the Pd- and Pt-substituted complexes [6,37,51,58].

From another point of view, the extremely fast relaxation of the excited state in Ni-BChla may result from a peculiar topology of the potential energy surface resulting from the strong bonding between the Ni^{2+} ion and the central nitrogens. If there are two electronic states of very similar energies (i.e. being pseudo-degenerated) located in the range of excitation energy, then due to vibronic interactions a saddle-shaped area can be formed on the potential energy surface. This corresponds to a crossing of the potential energy surfaces of a minimum of one normal vibration with a maximum of another one. The excitation localized in the potential having minimum "falls down" due to IC to the bottom of the potential where the structure of surface has maximum for the other potential in the other vibration, causing the excitation to disappear instantaneously.

In the LH1 antenna, the Ni-substituted pigment is strongly excitonically-coupled to other molecules that form the B880 compliment in the antenna [19]. Due to excitonic interactions, the S_1 state energy of the pigments forming LH1 ($\lambda_{max} = 875$ nm) is lowered from 12,820 cm^{-1} (free pigment) to 11,430 cm^{-1}. Apparently, this low energy transition in Ni-BChla is very effectively coupled to the rapid deactivation channel in this molecule whereas slower deexcitation pathways present in free Ni-BChla cannot be populated. Very likely, this is due to a fixed geometry (and symmetry) of the Ni-BChla molecules bound to the protein matrix. For the pigment in solution the situation is dynamic and several deactivation pathways can be active, depending on the momentary symmetry of the complex [8].

The results of the present analysis of the properties of Ni-substituted Chls can be summarized as follows. The excited state characteristics of complexes of transition metal ions with macrocyclic tetrapyrroles are strongly determined by local symmetry of the chelator. In the ligand field of the D_{4h} symmetry (unsubstituted porphyrins) the wavefunctions of the π-electron system and the central metal electrons are well separated whereas in the C_{2h}/C_2 symmetry (chlorophylls and bacteriochlorophylls) the respective electron systems strongly interact. It implies that in this type of complexes the local symmetry is decisive and must always be precisely determined. Consequently, any generalizations based on the systems of higher symmetries have to be applied very cautiously to the ones of lower symmetry. This is very well manifested in peculiar features of Ni-substituted (B)Chls, in particular in their extremely short lived excited states and 100% efficient excitation-to-heat-conversion, which can be explained by the formation of a strong three-center bond between Ni^{2+} ion and nitrogens in the central binding pocket of Chls. These characteristics render the Ni-substituted Chls a new class of excellent photocalorimetric references.

Acknowledgements

The work was supported in part by the National Science Center (2011–2012) and Poznan University of Technology (to J.Ł.), grant no. 0519/B/P01/2011/40 (to A.S.), and by a grant from the Foundation for Polish Science (TEAM/2010-5/3) (to L.F.). B.J. acknowledges a Ph.D. scholarship for students specializing in majors strategic for Wielkopolska's development (POKL Sub-measure 8.2.2, co-financed by European Union under the European Social Fund). The Faculty of Biochemistry, Biophysics and Biotechnology of the Jagiellonian University is a beneficiary of structural funds from the European Union (grant no: POIG.02.01.00-12-064/08—"Molecular biotechnology for health").

References

[1] J.J. Katz, H.H. Strain, D.L. Leussing, R.C. Dougherty, Chlorophyll–ligand interactions from nuclear magnetic resonance studies, J. Am. Chem. Soc. 90 (1968) 784–791.
[2] T.A. Evans, J.J. Katz, Evidence for 5- and 6-coordinated magnesium in bacteriochlorophyll a from visible absorption spectroscopy, Biochim. Biophys. Acta 396 (1975) 414–426.
[3] A. Drzewiecka-Matuszek, A. Skalna, A. Karocki, G. Stochel, L. Fiedor, Effects of heavy central metal on the ground and excited states of chlorophyll, J. Biol. Inorg. Chem. 10 (2005) 453–462.
[4] L. Fiedor, A. Kania, B. Mysliwa-Kurdziel, G. Stochel, Understanding chlorophylls: central magnesium and phytyl as structural determinants, Biochim. Biophys. Acta 1777 (2008) 1491–1500.
[5] T. Watanabe, K. Machida, H. Suzuki, M. Kobayashi, K. Honda, Photoelectrochemistry of metallochlorophylls, Coord. Chem. Rev. 64 (1985) 207–224.
[6] K. Teuchner, H. Stiel, D. Leupold, A. Scherz, D. Noy, I. Simonin, G. Hartwich, H. Scheer, Fluorescence and the excited state absorption in modified pigments of bacterial photosynthesis. A comparative study of metal-substituted bacteriochlorophylls a, J. Lumin. 72–74 (1997) 612–614.
[7] G. Hartwich, L. Fiedor, I. Simonin, E. Cmiel, W. Schäfer, D. Noy, A. Scherz, H. Scheer, Metal-substituted bacteriochlorophylls. 1. Preparation and influence of metal and coordination on spectra, J. Am. Chem. Soc. 120 (1998) 3675–3683.
[8] C. Musewald, G. Hartwich, H. Lossau, P. Gilch, F. Pöllinger-Dammer, H. Scheer, M.E. Michel-Beyerle, Ultrafast photophysics and photochemistry of [Ni]-bacteriochlorophyll a, J. Phys. Chem. 103 (1999) 7055–7060.
[9] H. Küpper, R. Dedic, A. Svoboda, J. Hala, P.M.H. Kroneck, Kinetics and efficiency of excitation transfer from chlorophylls, their heavy metal-substituted derivatives, and pheophytins to singlet oxygen, Biochim. Biophys. Acta 1572 (2002) 107–113.
[10] H. Küpper, F.C. Küpper, M. Spiller, [Heavy metal]-Chlorophylls formed in vivo during metal stress and degradation products formed during digestion, extraction and storage of plant material, in: B. Grimm, R.J. Porra, W. Rüdiger, H. Scheer (Eds.), Chlorophylls and Bacteriochlorophylls, vol. 25, Springer, Dordrecht, 2006, pp. 67–77.
[11] D. Eastwood, M. Gouterman, Porphyrins XVIII. Luminescence of (Co), (Ni), Pd, Pt complexes, J. Mol. Spectrosc. 35 (1970) 359–375.
[12] A. Harriman, Luminescence of porphyrins and metalloporphyrins. Part 3.—Heavy-atom effects, J. Chem. Soc. Faraday Trans. 2 (77) (1981) 1281–1291.
[13] C. Tanielian, C. Wolff, Determination of the parameters controlling singlet oxygen production via oxygen and heavy-atom enhancement of triplet yields, J. Phys. Chem. 99 (1995) 9831–9837.
[14] E.G. Azenha, A.C. Serra, M. Pineiro, M.M. Pereira, J.S. de Melo, L.G. Arnaut, S.J. Formosinho, A.M.d.A.R. Gonsalves, Heavy-atom effects on metalloporphyrins and polyhalogenated porphyrins, Chem. Phys. 280 (2002) 177–190.
[15] A. Brandis, Y. Salomon, A. Scherz, Bacteriochlorophyll sensitizers in photodynamic therapy, in: B. Grimm, R.J. Porra, W. Rüdiger, H. Scheer (Eds.), Chlorophylls and Bacteriochlorophylls, vol. 25, Springer, Dordrecht, 2006, pp. 485–494.
[16] A. Brandis, Y. Salomon, A. Scherz, Chlorophyll sensitizers in photodynamic therapy, in: B. Grimm, R.J. Porra, W. Rüdiger, H. Scheer (Eds.), Chlorophylls and Bacteriochlorophylls, vol. 25, Springer, Dordrecht, 2006, pp. 461–483.

[17] N.V. Koudinova, J.H. Pinthus, A. Brandis, O. Brenner, P. Bendel, J. Ramon, Z. Eshhar, A. Scherz, Y. Salomon, Photodynamic therapy with Pd-bacteriopheophorbide (Tookad): successful in vivo treatment of human prostatic small cell carcinoma xenographs, Int. J. Cancer 104 (2003) 782–789.
[18] O. Mazor, A. Brandis, V. Plaks, E. Neumark, V. Rosenbach-Belkin, Y. Salomon, A. Scherz, WST11, a novel water-soluble bacteriochlorophyll derivative; cellular uptake, pharmacokinetics, biodistribution and vascular-targeted photodynamic activity using melanoma tumors as a model, Photochem. Photobiol. 81 (2005) 342–351.
[19] L. Fiedor, H. Scheer, C.N. Hunter, F. Tschirschwitz, B. Voigt, J. Ehlert, E. Nibbering, D. Leupold, T. Elsaesser, Introduction of a 60 fs deactivation channel in the photosynthetic antenna LH1 by Ni-bacteriopheophytin a, Chem. Phys. Lett. 319 (2000) 145–152.
[20] L. Fiedor, D. Leupold, K. Teuchner, B. Voigt, C.N. Hunter, A. Scherz, H. Scheer, Excitation trap approach to analyze size and pigment–pigment coupling: reconstitution of LH1 antenna of *Rhodobacter sphaeroides* with Ni-substituted bacteriochlorophyll, Biochemistry 40 (2001) 3737–3747.
[21] C.M. Drain, C. Kirmaier, C.J. Medforth, D.J. Nurco, K.M. Smith, D. Holten, Dynamic photophysical properties of conformationally distorted nickel porphyrins. 1. Nickel(II) dodecaphenylporphyrin, J. Phys. Chem. 100 (1996) 11984–11993.
[22] H.S. Eom, S.C. Jeoung, D. Kim, J.-H. Ha, Y.-R. Kim, Ultrafast vibrational relaxation and ligand photodissociation/photodiassociation processes of nickel(II) porphyrins in the condensed phase, J. Phys. Chem. A 101 (1997) 3661–3669.
[23] C.M. Drain, S. Gentemann, J.A. Roberts, N.Y. Nelson, C.J. Medforth, M.C. Simpson, K.M. Smith, J. Fajer, J.A. Shelnutt, D. Holten, Picosecond to microsecond photodynamics of a nonplanar nickel porphyrin: solvent dielectric and temperature effects, J. Am. Chem. Soc. 120 (1998) 3781–3791.
[24] A.V. Zamyatin, A.V. Gusev, M.A.J. Rodgers, Two-pump-one-probe femtosecond studies of Ni(II) porphyrins excited states, J. Am. Chem. Soc. 126 (2004) 15934–15935.
[25] X. Zhang, E.C. Wasinger, A.Z. Muresan, K. Attenkofer, G. Jennings, J.S. Lindsey, L.-X. Chen, Ultrafast stimulated emission and structural dynamics in nickel porphyrins, J. Phys. Chem. A 111 (2007) 11736–11742.
[26] P. Gilch, C. Musewald, M.E. Michel-Beyerle, Magnetic field dependent picosecond intersystem crossing. The role of molecular symmetry, Chem. Phys. Lett. 325 (2000) 39–45.
[27] G. Hartwich, M. Friese, H. Scheer, A. Ogrodnik, M.E. Michel-Beyerle, Ultrafast internal conversion in 13^2-OH-Ni-bacteriochlorophyll in reaction centres of *Rhodobacter sphaeroides* R26, Chem. Phys. 197 (1995) 423–434.
[28] K. Iriyama, N. Ogura, A. Takamiya, A simple method for extraction and partial purification of chlorophyll from plant material, using dioxane, J. Biochem. 76 (1974) 901–904.
[29] T. Omata, N. Murata, Preparation of chlorophyll a, chlorophyll b and bacteriochlorophyll a by column chromatography with DEAE-Sepharose CL-6B and Sepharose CL-6B, Plant Cell Physiol. 24 (1983) 1093–1100.
[30] L. Fiedor, V. Rosenbach-Belkin, A. Scherz, The stereospecific interaction between chlorophylls and chlorophyllase. Possible implication for chlorophyll biosynthesis and degradation, J. Biol. Chem. 267 (1992) 22043–22047.
[31] T. Gensch, S.E. Braslavsky, Volume changes related to triplet formation of water-soluble porphyrins. A laser-induced optoacoustic spectroscopy (LIOAS) study, J. Phys. Chem. 101 (1997) 101–108.
[32] C. Marti, S. Nonell, M. Nicolaus, T. Torres, Photophysical properties of natural and cationic tetrapyridinoporphyrazines, Photochem. Photobiol. 71 (2000) 53–59.
[33] S.E. Braslavsky, G.E. Heibel, Time-resolved photothermal and photoacoustic methods applied to photoinduced processes in solution, Chem. Rev. 92 (1992) 1381–1410.
[34] C. Marti, O. Jürgens, O. Cuenca, M. Casals, S. Nonell, Aromatic ketones as standards for singlet molecular oxygen O_2 ($^1\Delta_g$) photosensitization. Time-resolved photoacoustic and near-IR emission studies, J. Photochem. Photobiol. A 97 (1996) 11–18.
[35] S. Krawczyk, The effects of hydrogen bonding and coordination interaction in visible absorption and vibrational spectra of chlorophyll a, Biochim. Biophys. Acta 976 (1989) 140–149.
[36] A. Kania, L. Fiedor, Steric control of bacteriochlorophyll ligation, J. Am. Chem. Soc. 128 (2006) 454–458.
[37] C. Musewald, G. Hartwich, F. Pöllinger-Dammer, H. Lossau, H. Scheer, M.E. Michel-Beyerle, Time-resolved spectral investigation of bacteriochlorophyll a and its transmetalated derivatives [Zn]-bacteriochlorophyll a and [Pd]-bacteriochlorophyll a, J. Phys. Chem. B 102 (1998) 8336–8342.
[38] S. Abbruzzetti, C. Viappiani, D.H. Murgida, R. Erra-Balsells, G.M. Bilmes, Non-toxic, water-soluble photocalorimetric reference compounds for UV and visible excitation, Chem. Phys. Lett. 304 (1999) 167–172.
[39] P. van Haver, L. Viaene, M. van der Auweraer, F.C. De Schryver, References for laser-induced opto-acoustic spectroscopy using UV excitation, J. Photochem. Photobiol. A 63 (1992) 265–277.
[40] L. Fiedor, A.A. Gorman, I. Hamblett, V. Rosenbach-Belkin, Y. Salomon, A. Scherz, I. Tregub, A pulsed laser and pulse radiolysis study of amphiphilic chlorophyll derivatives with PDT activity toward malignant melanoma, Photochem. Photobiol. 58 (1993) 506–511.
[41] J. Fiedor, L. Fiedor, N. Kammhuber, A. Scherz, H. Scheer, Photodynamics of the bacteriochlorophyll-carotenoid system. 1. Influence of central metal, solvent and β-carotene on photobleaching of bacteriochlorophyll derivatives, Photochem. Photobiol. 76 (2002) 145–152.
[42] A.P. Darmanyan, C.S. Foote, Solvent effects on singlet oxygen yield from n, π^* and π, π^* triplet carbonyl compounds, J. Phys. Chem. 97 (1993) 5032–5035.
[43] In: S.L. Murov, I. Carmichael, G.L. Hug (Eds.), Handbook of Photochemistry, Marcel Dekker, Inc., New York, 1993.
[44] S. Gentemann, C.J. Medforth, T.P. Forsyth, D.J. Nurco, K.M. Smith, J. Fajer, D. Holten, Photophysical properties of conformationally distorted metal-free porphyrins, Investig. J. Am. Chem. Soc. 116 (1994) 7363–7368.
[45] J.L. Retsek, S. Gentemann, C.J. Medforth, K.M. Smith, V.S. Chirvony, J. Fajer, D. Holten, Photoinduced evolution on the conformational landscape of nonplanar dodecaphenylporphyrin: picosecond relaxation dynamics in the $1(\pi, \pi^*)$ excited state, J. Phys. Chem. B 104 (2000) 6690–6693.
[46] P. Fita, C. Radzewicz, J. Waluk, Electronic and vibrational relaxation of porphycene in solution, J. Phys. Chem. A 112 (2008) 10753–10757.
[47] Ł. Orzeł, A. Kania, D. Rutkowska-Zbik, A. Susz, G. Stochel, L. Fiedor, Structural and electronic effects in the metalation of porphyrinoids. Theory and experiment, Inorg. Chem. 49 (2010) 7362–7371.
[48] H. Ryeng, A. Ghosh, Do nonplanar distortions of porphyrins bring about strongly red-shifted electronic spectra? Controversy, consensus, new developments, and relevance to chelatases, J. Am. Chem. Soc. 124 (2002) 8099–8103.
[49] S.A. Krasnikov, A.B. Preobrajenski, N.N. Sergeeva, M.M. Brzhezinskaya, M.A. Nestrov, A.A. Cafolla, M.O. Senge, A.S. Vinogradov, Electronic structure of Ni(II) porphyrins and phtalocyanine studied by soft X-ray absorption spectroscopy, Chem. Phys. 332 (2007) 318–324.
[50] P.M. Callahan, T.M. Cotton, Assignment of bacteriochlorophyll a ligation state from absorption and resonance Raman spectra, J. Am. Chem. Soc. 109 (1987) 7001–7007.
[51] T. Kobayashi, K.D. Straub, P.M. Rentzepis, Energy relaxation mechanism in Ni(II), Pd(II), Pt(II) and Zn(II) porphyrins, Photochem. Photobiol. 29 (1979) 925–931.
[52] E.W. Findsen, J.A. Shelnutt, M.R. Ondrias, Photodynamics of nickel porphyrins in noncoordinating solvents: characterization of d–d excited states using transient Raman spectroscopy, J. Phys. Chem. 92 (1988) 307–314.
[53] J.D. Petke, G.M. Maggiora, L.L. Shipman, R.E. Christoffersen, Stereoelectronic properties of photosynthetic and related systems — VI. *Ab initio* configuration interaction calculations on the ground state and lower excited singlet and triplet states of ethyl bacteriochlorophyllide-a and ethyl bacteriopheophorbide-a, Photochem. Photobiol. 32 (1980) 399–414.
[54] M.H. Vos, Ultrafast dynamics of ligands within heme proteins, Biochim. Biophys. Acta 1777 (2008) 15–31.
[55] D. Huppert, K.D. Straub, P.M. Rentzepis, Picosecond dynamics of iron proteins, Proc. Natl. Acad. Sci. U. S. A. 74 (1977) 4139–4143.
[56] A. Harriman, Luminescence of porphyrins and metalloporphyrins. Part 2.—Copper(II), chromium(III), manganese(III), iron(II) and iron(III) porphyrins, J. Chem. Soc. Faraday Trans. 1 (77) (1981) 369–377.
[57] J. Rodriguez, D.J. Holten, Ultrafast vibrational dynamics of a photoexcited metalloporphyrin, J. Chem. Phys. 91 (1989) 3525–3531.
[58] J.B. Callis, M. Gouterman, Y.M. Jones, B.H. Henderson, Porphyrins XXII: fast fluorescence, delayed fluorescence, and quasiline structure in palladium and platinum complexes, J. Mol. Spectrosc. 39 (1970) 410–420.